REPORT DOCUMENTATION PAGE

AFRL-SR-BL-TR-02-

0251

1. AGENCY USE ONLY *(Leave blank)*	2. REPORT DATE	3. REPORT TYPE AND DATES COVERED
		01 Sep 97 to 31 May 01 FINAL

4. TITLE AND SUBTITLE
97-AASERT Photo-Hall Characterization of Semiconductor Matrices with Disordered Particulates

5. FUNDING NUMBERS
61103D
3484/TS

6. AUTHOR(S)
Prof. Melloch

7. PERFORMING ORGANIZATION NAME(S) AND ADDRESS(ES)
Purdue Research Foundation University
1063 Hovde Hall
West Lafayette, IN 47907-1063

8. PERFORMING ORGANIZATION REPORT NUMBER

9. SPONSORING/MONITORING AGENCY NAME(S) AND ADDRESS(ES)
AFOSR/NE
801 North Randolph Street Rm 732
Arlington, VA 22203-1977

10. SPONSORING/MONITORING AGENCY REPORT NUMBER

F49620-97-1-0377

11. SUPPLEMENTARY NOTES

AIR FORCE OFFICE OF SCIENTIFIC RESEARCH (AFOSR)
NOTICE OF TRANS...
HAS BEEN REVIEWED AND IS APPROVED FOR PUBLIC RELEASE
LAW AFR 190-12. DISTRIBUTION IS UNLIMITED.

12a. DISTRIBUTION AVAILABILITY STATEMENT
APPROVAL FOR PUBLIC RELEASED; DISTRIBUTION UNLIMITED

12b. DISTRIBUTION CODE

13. ABSTRACT *(Maximum 200 words)*

1. Mobility of Carriers in LTG-GaAs:
GaAs epilayers containing arsenic precipitates are semi-insulating because of a lack of carriers. Therefore a direct measurement cannot be made of the mobility. When these materials are used as photoconductors, light produces electron-hole pairs.
2. Large-Area, High-Speed Photodetector:
Recently, large-area photodetectors have become very important in high-speed fiber communications. Large area detectors are essential to the success of plastic-fiber optical networks.

20020221 056

14. SUBJECT TERMS		15. NUMBER OF PAGES
		16. PRICE CODE

17. SECURITY CLASSIFICATION OF REPORT	18. SECURITY CLASSIFICATION OF THIS PAGE	19. SECURITY CLASSIFICATION OF ABSTRACT	20. LIMITATION OF ABSTRACT
UNCLASSIFIED	UNCLASSIFIED	UNCLASSIFIED	UL

Final Report

I

Photo-Hall Characterization of Semiconductor Matrices with Disordered Particulates

Michael R. Melloch
School of Electrical and Computer Engineering
Purdue University
West Lafayette, IN 47907-1285

Personnel Supported

Graduate Students: Jason Henning, Ivan Milos, and Brian Johnson

Undergraduate student: Michael Hauser

Accomplishments/New Findings:

1. Mobility of Carriers in LTG-GaAs

GaAs epilayers containing arsenic precipitates are semi-insulating because of a lack of carriers. Therefore a direct measurement cannot be made of the mobility. When these materials are used as photoconductors, light produces electron-hole pairs. It is the mobility of these photogenerated electrons that determines how quickly the photoconductor turns on. During the first year of this program we developed a photo-Hall technique to measure the mobility of electrons in LTG-materials. A standard Hall bar is fabricated using wet-etching. The photomask that was used for wet-etching the Hall bar is used to lift-off metal in the bottom of the trenches. This prevents photogeneration of unwanted carriers outside the active region of the Hall bar that might leak back into the Hall bar structure. When the bar is uniformly illuminated with light, a steady-state electron-hole population exists in the bar. By varying the light intensity the electron density can be varied. The samples are packaged so that they can be placed in a magnetic field. A Hall measurement can then be made to determine the electron density and the corresponding mobility. Our initial measurements are shown in the following figure.
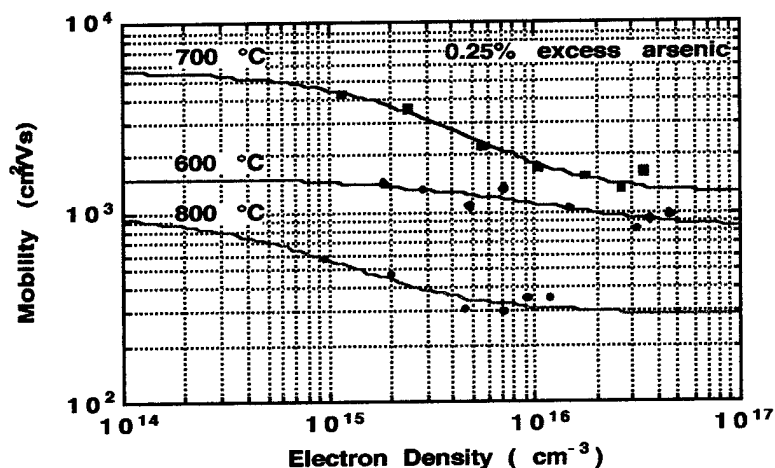

Figure 1. Results of photo-Hall measurements of LTG-GaAs.

The epilayer contained 0.25% excess arsenic and Hall bars were made from material annealed for 30 seconds at 600, 700, and 800 °C. There is clearly an initial improvement in mobility with anneal

as the point defects are removed from the as-grown material. However, there is clearly going to be an optimum anneal as the mobility begins to decrease again at an anneal of 800 °C. The electron mobility decreases with increase in photo-generated electron density because the more massive holes, which are also produced by the photogeneration, effectively act as ionized acceptors scattering the lighter electrons.

2. Large-Area, High-Speed Photodetector

Recently, large-area photodetectors have become very important in high-speed fiber communications. Large area detectors are essential to the success of plastic-fiber optical networks. Plastic fibers are cost-effective in short-range communication and have a core diameter of 300 μm. In order to achieve a gigabit communication link, the critical component is a high-speed large-area detector. A planar metal-semiconductor-metal photodetector (MSM-PD) exhibits a lower capacitance per unit area than a vertical p-i-n structure with better noise-characteristics [1], which is very important in a high-speed fiber-optic link. The MSM-PD is easier to fabricate and is easily integrated in an optoelectronic integrated circuit (OEIC). These properties make it an ideal candidate for application as a large-area detector.

The result of low-temperature growth is the inclusion of excess arsenic in the composite, which then shortens the carrier lifetime [2]. We have previously mapped this material space as a function of growth temperature and post-growth annealing. Consequently, we can choose the lifetime property required for a given application, while maintaining high mobility and high resistivity. This has then resulted in intermediate temperature grown GaAs (ITG-GaAs), where the growth temperature of the semiconductor composite is in between that of traditional GaAs and typical LTG temperatures. Subsequently, we can tailor the carrier lifetime of the light absorption region to be slightly longer than the transit-time between the electrodes. Such control gets rid of the long hole-tail while averting intersymbol interference, which is a characteristic of the impulse response of MSM-PDs. Thus, the speed of the detector is improved without significantly reducing the responsivity. We report the first large-area MSM-PD (400 μm X 400 μm) with a full width at half-maximum (FWHM) of 86 ps (4 GHz bandwidth). We present a detailed study of large-area MSM-PDs with various finger-spacings including temporal responses, dark currents and the dc responsivities. We thus show that ITG-GaAs is an excellent material for the fabrication of large-area MSM-PDs.

The devices reported here consist of a 0.5 μm GaAs buffer-layer grown by molecular beam epitaxy on a semi-insulating GaAs substrate. This was followed by 30 nm of $Al_{0.3}Ga_{0.7}As$ and then a 1 μm thick GaAs light-absorption layer was grown at 400°C. Another $Al_{0.3}Ga_{0.7}As$ layer, 30 nm thick was grown to improve the surface mobility. The device was then capped with an $Al_{0.5}Ga_{0.5}As$ layer. The samples were annealed at a temperature of 800°C.

The layers were nominally undoped. An antireflection coating of SiN_x was also deposited to improve the responsivity of the device by coupling more of the light into the detector. The devices were composed of interdigitated 1 μm–wide Ti-Au electrodes with spacing varying from 2 μm to 6 μm. The devices had a square geometry and an active area of 400 μm X 400 μm (160,000 μm²). Fabrication was done using standard contact lithography and a metal lift-off process. The fingers were contacted using ground-signal-ground pads, 100 μm X 100 μm in size. These were deposited using image-reversal photolithography and by a metal lift-off.

Near infrared (λ = 800 nm) 125 fs pulses with a repetition rate of 76 MHz were obtained from a Coherent MIRA 900 mode-locked laser. These light pulses were then directed onto the on-wafer devices using a multi-mode fiber and light-wave probe arrangement. The devices were electrically contacted using a ground-signal-ground microwave probe, SMA cable and bias-tee assembly. The photocurrent was then measured as a function of time. The dark current and dc responsivity measurements were also made and the results are presented in the next section.

The dark current as a function of voltage was measured for the MSM-PDs. A typical dark IV curve for a 160,000 μm² area, 5 μm spacing device is shown in Figure 2. The MSM-PDs had very low dark current densities varying from 4.4 fA/μm² for the 6 μm spacing device to 5.6 fA/μm² for the 3 μm spacing device for a bias of 10V. In comparison, the dark current of HTG-GaAs MSM-PDs ranged from 0.92 fA/μm² to 5.38 fA/μm². Recent work has shown that dark current densities of this magnitude can be expected for ITG-GaAs MSM-PDs [4]. The dark currents tend to increase with increasing bias, because of the image-force lowering of the Schottky barrier.

The photoresponse of the MSM-PDs were measured using a 820 nm CW laser. The laser light was regulated using an optical fiber attenuator. I-V curve measurements were then made for varying light powers and the photocurrent of a 5 μm finger-spacing MSM-PD is plotted in Figure 2. The photocurrent is two orders of magnitude greater than the dark current even at low light intensities(1 μW). In Figure 2, we can also see a clear positive shift of the flat-band knee with increase in illumination intensity. This is attributed to the increase in space-charge [5], which tends to screen out the electric field. Figure 3 makes a comparison of the responsivities (photocurrent/light input power) of ITG-GaAs MSM-PDs and HTG-GaAs MSM-PDs. For a bias of 10V and a light-input power of 100 μW, the responsivities of ITG-GaAs devices were found to be in the range of 0.12 A/W to 0.18 A/W. In comparison, the responsivites of the HTG-GaAs devices were found to be in the range of 0.35 A/W to 0.42 A/W. The ITG GaAs MSMs showed a decrease in responsivity with an increase in finger spacing, which is counter-intuitive when considering shadowing effects. However, the field strength is diminished by the larger finger spacing. This decrease is enhanced by field screening and non-uniformity due to the arsenic precipitates. This is absent in the HTG-GaAs devices which display typical responses. Moreover, the arsenic precipitates act as recombination centers, resulting in fewer carriers being available to

transit out of the device. Both these effects reduce the responsivity of the device. As seen in Figure 3, the photodetectors had a linear response over most of the range of optical powers (10 µW to 1 mW). However, at low light intensities, there was a sharp increase in responsivity. At higher light intensities, charge pile-up occurs at the contacts because of the increased rate of carrier-generation[6]. This carrier-crowding leads to an increase in scattering of the carriers. At lower intensities, this carrier-crowding is absent and consequently there is an increase in the responsivity.

The temporal responses of the MSM-PDs were measured using 125 fs light pulses at a wavelength of 800 nm. A DC bias of 10V was applied and measurements were made at different average light input powers. The pulse response of a MSM-PD with a finger-spacing of 6 µm, has a FWHM of 86 ps and a fall time of 112 ps (Fig.4). In the authors' knowledge, this is the first report of a large-area (160,000 µm²) photodetector with a bandwidth of 4 GHz.

The fall-time of the devices increased with a decrease in finger spacing. The capacitance of a planar MSM-PD also increases with a decrease in finger spacing [7]. This implies that the devices are operating in the capacitance-limited regime. This view is reinforced by the increase in FWHM of the device with a decrease in finger-spacing (86 ps for a 6 µm device to 194 ps for a 2 µm device). However, there is a dramatic improvement in the fall-time of the device because of the suppression of the hole-tail, which is a characteristic of the impulse response of MSM-PDs (Fig.5). The fall-time of a 6 µm spacing ITG-GaAs MSM-PD is 112 ps at an average light input power of 100 µW and 10 V bias. The response of a similar size normal-temperature grown GaAs MSM-PD at the same light input power had a fall-time of 383 ps. The difference is even more pronounced at higher average light powers (1 mW), as seen in Figure 5. This dramatic decrease in the fall time of the detector can be attributed to the use of the intermediate-temperature grown material to control the lifetime in the material [2]. The device capacitance of the ITG-GaAs device and the HTG-GaAs device were measured and found to be 1.6 pF and 1.2 pF respectively, indicating that the difference in fall-time cannot be due to the capacitance. In normal-GaAs, the long hole-tail is caused by the generation of carriers deep in the light-absorption region of the device. This region of the device has low field intensities. Hence, the carriers (especially the holes) take a long time in recombining or transiting out of the device. This leads to the long hole-tail in the impulse response of the device. Now, in ITG-GaAs, we can control the carrier-lifetime of the device to be slightly longer than the transit-time between electrodes. Therefore, carriers generated deeper in the light-absorption region quickly recombine, leading to a suppression of the hole-tail as seen in Figure 5. At the same time, this ensures that enough carriers make it to the electrodes resulting in a good responsivity for the device. Thus, carrier-lifetime control by the use of ITG-GaAs can be used to improve the performance of large-area MSM-PDs.
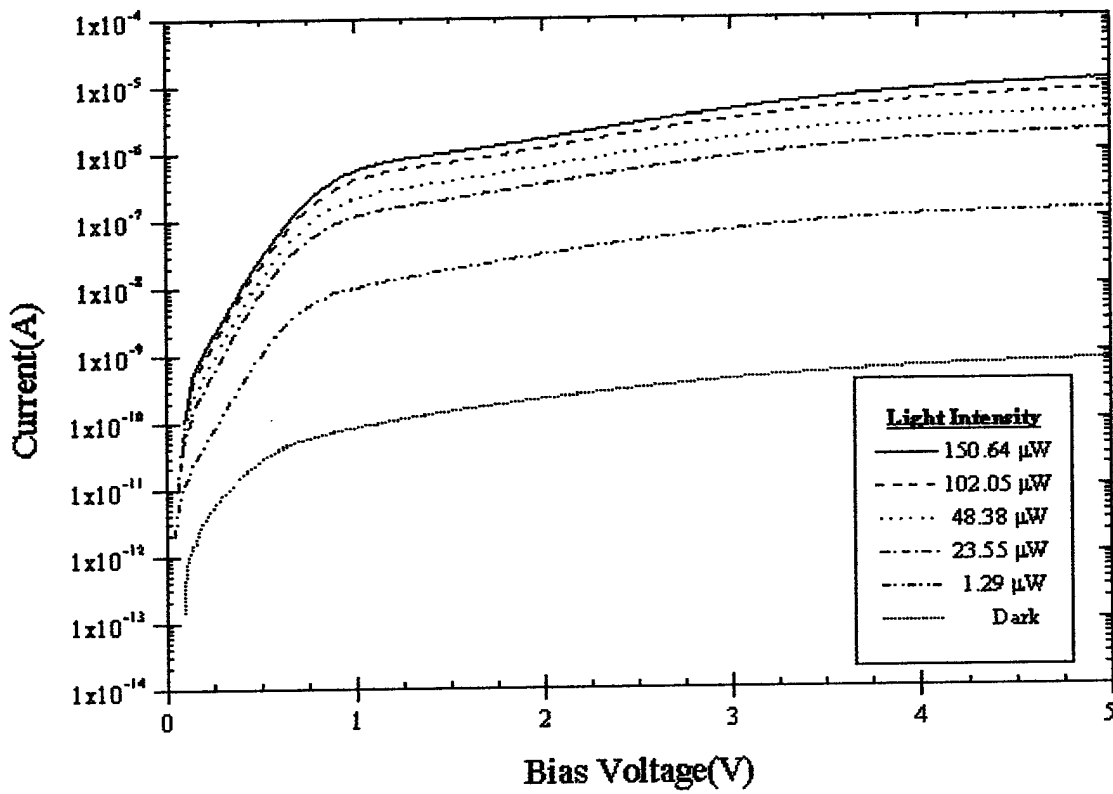
Fig.2. I-V Characteristics of a MSM-PD for different light input powers. Area = 160,000 μm^2, Finger spacing = 5 μm; Wavelength (λ) = 820 nm; Light powers varying from 1.29 μW to 150.64 μW. The dark current of the device is also shown.
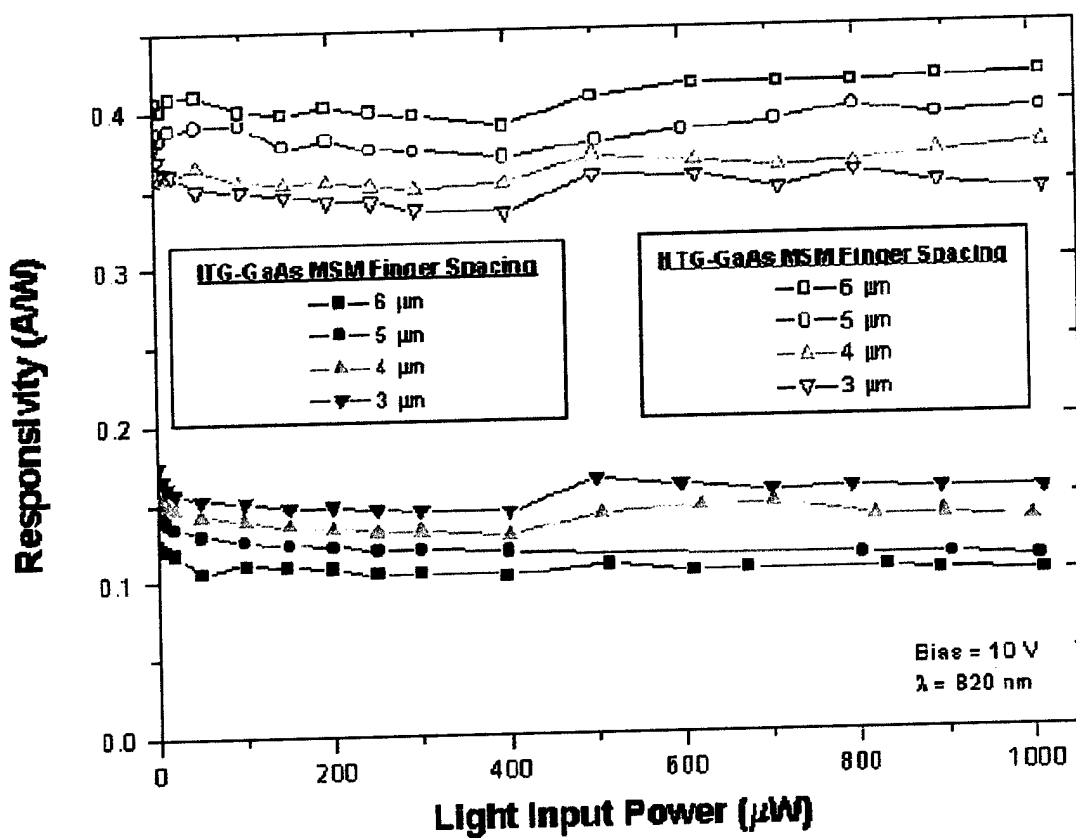
Fig.3. Responsivity of ITG-GaAs MSM-PDs and HTG-GaAs MSM-PDs as a function of light-power and finger-spacing. Area = 160,000 μm²; Bias = 10 V; Wavelength (λ) = 820 nm; Finger spacing varies from 3 μm to 6 μm.

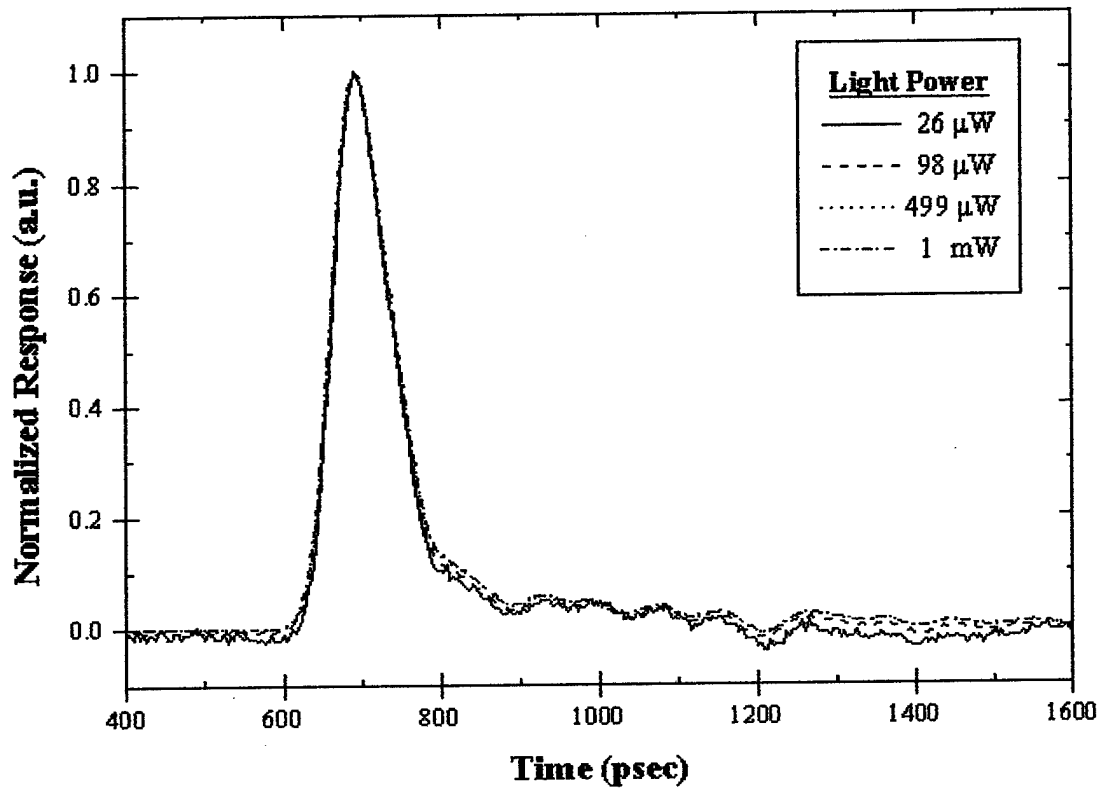**Fig.4.** Impulse response of a large-area (160,000 μm^2) MSM-PD for different average light powers. Finger spacing = 6 μm; Wavelength (λ) = 800 nm; Bias = 10 V. The measured FWHM at 28 μW light power was 86 ps.
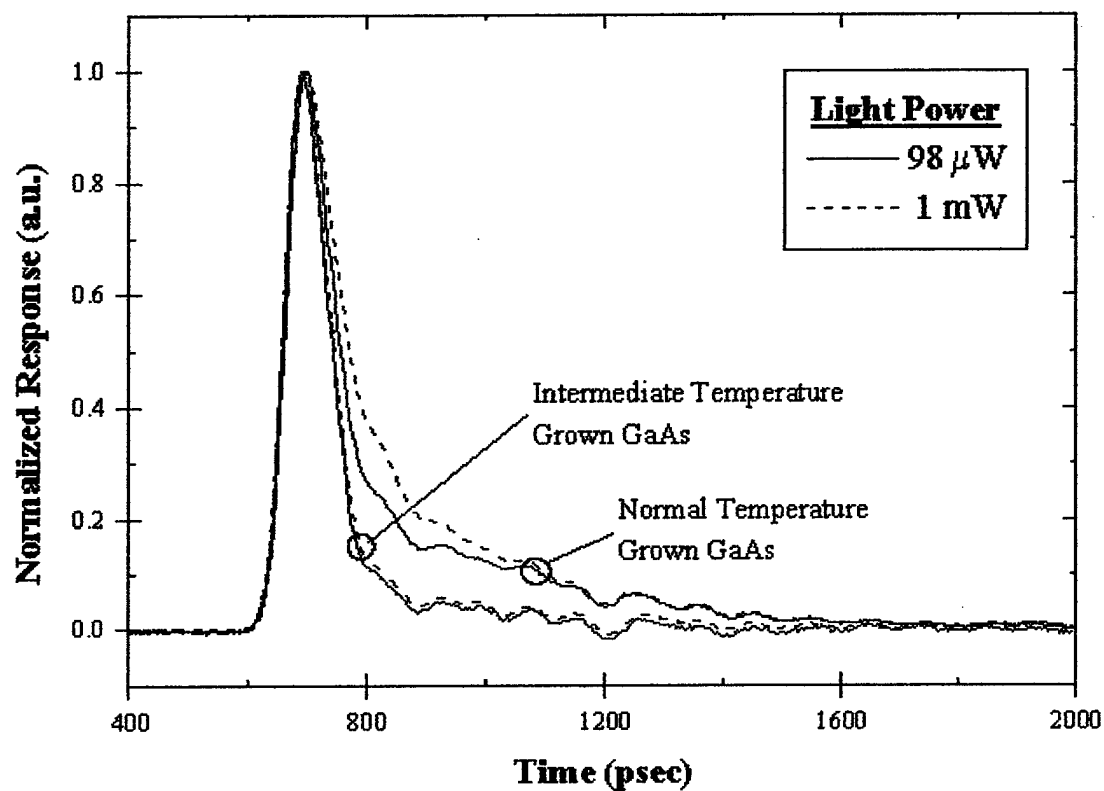
Fig.5. Comparison of the impulse response of ITG-GaAs and HTG-GaAs MSM-PD. Area = 160,000 μm^2; Finger spacing = 6 μm; Wavelength (λ) = 800 nm; Bias = 10 V. Rise times were 112 ps (ITG-GaAs) and 383 ps (HTG-GaAs).